Radial Characterization of the Electron Energy Distribution in a Helicon Source Terminated by a Double Layer

doi: 10.1063/1.2959137

Radial characterization of the electron energy distribution in a helicon source terminated by a double layer

Kazunori Takahashi,[1,2,a)] Christine Charles,[1] Rod Boswell,[1] and Rikizo Hatakeyama[2]
[1]*Space Plasma, Power and Propulsion Group, Research School of Physical Sciences and Engineering, The Australian National University, Canberra ACT 0200, Australia*
[2]*Department of Electronic Engineering, Tohoku University, Sendai 980-8579, Japan*

(Received 13 May 2008; accepted 26 June 2008; published online 25 July 2008)

Electron energy probability functions (EEPFs) are measured across the radius ($0 \leqslant r < 6.85$ cm) of a low pressure (0.3 mTorr) helicon plasma source terminated by a current-free double layer. The source field of about 130 G is generated using a Helmholtz coil pair and the radio frequency (rf) power is maintained at 250 W. All EEPFs exhibit a distribution with a temperature $T_{e\ \mathrm{bulk}}$ out to a break energy $\varepsilon_{\mathrm{break}}$ and a relatively depleted distribution for higher energies with a lower temperature $T_{e\ \mathrm{tail}}$. $T_{e\ \mathrm{bulk}}$ and $T_{e\ \mathrm{tail}}$ are about 8 eV and 5 eV, respectively, for $r < 4$ cm and increase up to about 14 eV and 9 eV near the source wall, i.e., near the rf antenna. $\varepsilon_{\mathrm{break}}$ is found to correspond to the potential drop of the double layer for the central part of the source and to the sheath potential near the wall. © *2008 American Institute of Physics*. [DOI: 10.1063/1.2959137]

Laboratory double layers (DLs) have been recently reported in inductively coupled magnetized expanding radio frequency (rf) plasmas.[1–6] The role of electric DLs in space plasmas such as the Aurora and the Solar corona[7,8] and their application to a new type of plasma thruster have been discussed.[9] One dimensional (1D) particle-in-cell (PIC) simulation with three dimensional (3D) collision treatment of an inductively coupled expanding plasma containing a DL has shown that the electron energy distribution function (EEDF) in the source consists of a Maxwellian with a depleted tail, in good agreement with the most recent results.[10,11] The break energy separating the Maxwellian from the depleted tail was found to be correlated to the DL potential drop. In low pressure nonexpanding and nonmagnetized plasmas, similar results were found experimentally[12] and by simulation[10] with the break energy corresponding to the wall sheath potential. A theory based on low pressure diffusion models in the absence of a magnetic field has shown the existence of DL solutions using a spatially uniform and constant electron temperature T_e in the helicon source with the addition of an electron beam.[13–15] Although this theory agrees well with the measured DL potential drop versus operating pressure for a variety of gases,[9,16] it is based on the assumption of no magnetic field and of a simplified EEDF. Other DL models with the inclusion of a diverging magnetic field also rely on a simplified EEDF.[17,18] The role of the magnetic field and of the rf antenna geometry on the transition from a simple expansion to a DL containing expansion has been recently shown experimentally,[6,19] suggesting that radial effects within the helicon source need to be investigated.

Here we report on the first measurements of the radial electron energy probability functions (EEPF) in a helicon plasma having a double layer as a boundary condition at its open end. The CHI-KUNG experimental set up is shown in Fig. 1. It has been previously described[20] and consists of a 31-cm-long, 13.7-cm-internal-diameter helicon source terminated by a glass plate at one end and contiguously attached to a grounded 29.4-cm-long, 31.8-cm-internal-diameter vacuum chamber at the other end. The system is pumped down to a base pressure of $\sim 2 \times 10^{-6}$ Torr using a turbomolecular/rotary pumping system connected to the side of the diffusion chamber. The gas inlet is connected to a chamber sideport and the pressure is measured using a baratron gauge and an ion gauge also attached to a chamber sideport. The source consists of a Pyrex tube surrounded by a double-saddle field rf antenna extending between $z=3$ cm and $z=21$ cm (z is the reactor's axis and $z=30$ cm is the source/chamber interface) and fed from a rf matching network/generator system operating at 13.56 MHz. The rf power is presently maintained at 250 W. Surrounding the tube and antenna, two solenoids centered at $z=3$ cm (740 turns) and $z=21$ cm (700 turns), respectively, are used to create a divergent magnetic field near the source exit. In this study the solenoids are fed by equal currents of 6 A and the generated magnetic field decreases from about 130 G in the source to about 10 G in the middle of the diffusion chamber.[6] The argon gas pressure is maintained at about 0.3 mTorr. The present operating conditions lead to the spontaneous formation of a current-free double layer near the open end of the source at $z=25$ cm.[2]

A rf-compensated 3 mm-long 0.25 mm-diam cylindrical Langmuir probe (CP) previously described[11,21] is placed perpendicularly to the axis at $z=17$ cm, i.e., about 8 cm upstream of the DL ($z=25$ cm) to measure the plasma density, plasma potential, and electron temperature. The probe voltage is swept and the current detected across a resistor; this signal is twice differentiated using an active analog circuit. We have found that it is not uncommon to be able to measure currents over at least 3 orders of magnitude which allows details of the EEPF to be closely examined. The probe enters

[a)]Permanent address: Department of Electrical and Electronic Engineering, Iwate University, Japan. Electronic mail: kazunori@iwate-u.ac.jp.

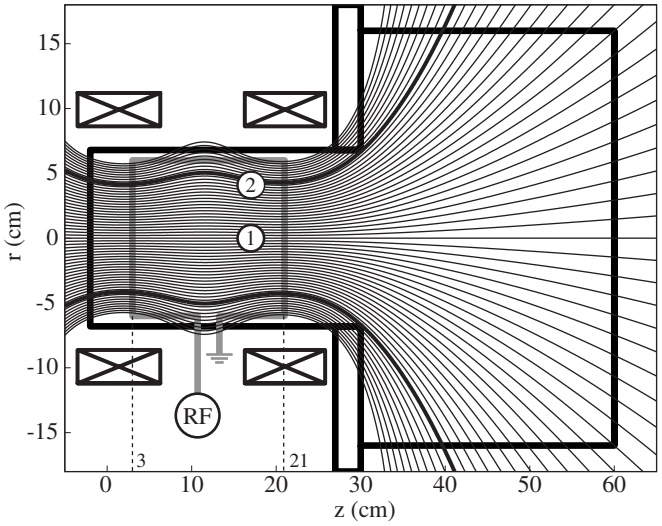

FIG. 1. Schematic of the helicon double layer CHI-KUNG reactor showing the axial solenoids and the magnetic field lines with 6 A in each solenoid. Circles 1 and 2 shown at $z=17$ cm, respectively, correspond to the rf compensated probe positions of Figs. 2(a) and 2(b).

the vacuum system through the metallic end plate of the chamber and has a "dog leg" that allows radial measurements when the probe is rotated. The internal tube radius is 6.85 cm. The magnetic field lines are shown in Fig. 1: The bold line delineates the field lines terminating on the source walls from the field lines terminating on the chamber walls. At $z=17$ cm it corresponds to a radius of about 4 cm. Two examples of EEPFs measured for a pressure of 0.3 mTorr and a rf power of 250 W at $r=0$ and $r=4$ cm are shown in Figs. 2(a) and 2(b), respectively.

At high energies both EEPFs show a depletion compared to a Maxwellian distribution fitted to the low energy electrons. In the center of the source at $r=0$ cm [Fig. 2(a)] the

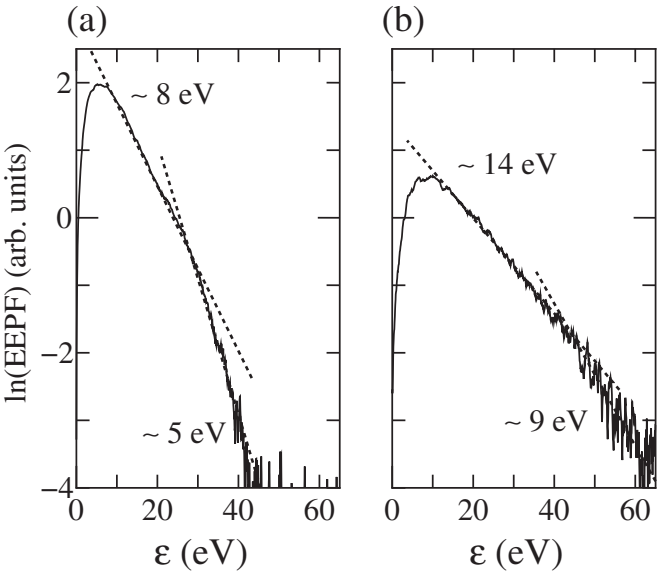

FIG. 2. EEPFs measured using the rf compensated Langmuir probe, respectively, positioned at (a) $(z,r)=(17\text{ cm},0\text{ cm})$ (circle 1 in Fig. 1) and at (b) $(z,r)=(17\text{ cm},4\text{ cm})$ (circle 2 in Fig. 1); operating conditions are 250 W rf power and 0.3 mTorr gas pressure.

break energy $\varepsilon_{\text{break}}$ where the depletion begins occurs at around 27 eV, which corresponds closely to the potential drop of the DL that has already been reported to be about 25 V.[2] Below the break the average energy of the electrons is 8 eV and above 5 eV. It should also be noted that if we consider that equal fluxes of ions and electrons are escaping from the source through the DL, then we would expect the amplitude of the double layer to be 5×5 eV (where 5 eV is the temperature of the escaping electrons, not the bulk) which it indeed is, where the fluxes of ions and electrons are described in Ref. 22 and lead to the potential drop of $5\times T_e$. The 5 eV population can move freely to the end of the chamber and return to the source, whereas the 8 eV population is trapped inside the source by the DL at the open end and the left-hand wall sheath at the other.

Close to the insulating source wall at $r=4$ cm [Fig. 2(b)] the break energy $\varepsilon_{\text{break}}$ occurs at about 45 eV and both electron populations are hotter with $T_{e\ \text{bulk}}$ being 14 eV and $T_{e\ \text{tail}}$ being 9 eV. In an earlier publication[10] it was shown that the break energy in an EEDF close to a wall reflects the potential of the wall sheath. The local plasma potential obtained from the second derivative zero crossing at $r=4$ cm is about 62 V and the wall potential measured (very approximately by actually contacting the probe to the wall) at the closed left end is 16 V. Thus, the sheath voltage on the floating wall can be estimated to be about 46 V, in good agreement with the break energy. Considering that the amplitude of the wall sheath is given by the energy of the escaping electrons, the slope of the EEPF above the break energy in Fig. 2(b) yields 9 eV for the average energy of the escaping electrons and so the equal flux criterion yields a wall sheath of (5×9) 45 V, once again in surprisingly good agreement with both the break energy and the estimate of (V_p-V_f).

In the inner region, for radii between −4 and +4 cm, the magnetic field lines intersect both ends of the vacuum vessel whereas for radii larger than 4 cm, the magnetic field lines only intersect the walls of the source (Fig. 1). As the electrons have a gyro diameter of about 1 mm and a collision mean free path of over a meter, they are tied very strongly to the magnetic field lines and the electrons in the inner region will suffer more collisions with the sheaths at the ends of the system than with the neutrals. Additionally, they will interact with any electric fields existing along the axis of the system. Those in the outer region cannot escape from the source and will collide with the sheaths on the insulating source walls.

It has become common practice to describe the slope of the EEPF as a temperature and while this is correct for a simple Maxwellian, for the more complicated EEPFs we present here we should use a phrase, such as, "the average electron energy for bulk electrons is 8 eV and for the tail electrons 5 eV." However, the custom of using temperature and energy interchangeably for describing (parts of) EEPFs is so widespread that we will also follow this simple (although not formally correct) nomenclature. That part of the EEPF with energies lower than the break energy we will refer to as $T_{e\ \text{bulk}}$ and that part with energies higher, $T_{e\ \text{tail}}$.

A detailed radial investigation was carried out using the Langmuir probe placed at $z=17$ cm and the results of the electron temperatures $T_{e\ \text{bulk}}$ and $T_{e\ \text{tail}}$ (bulk and tail, i.e.,

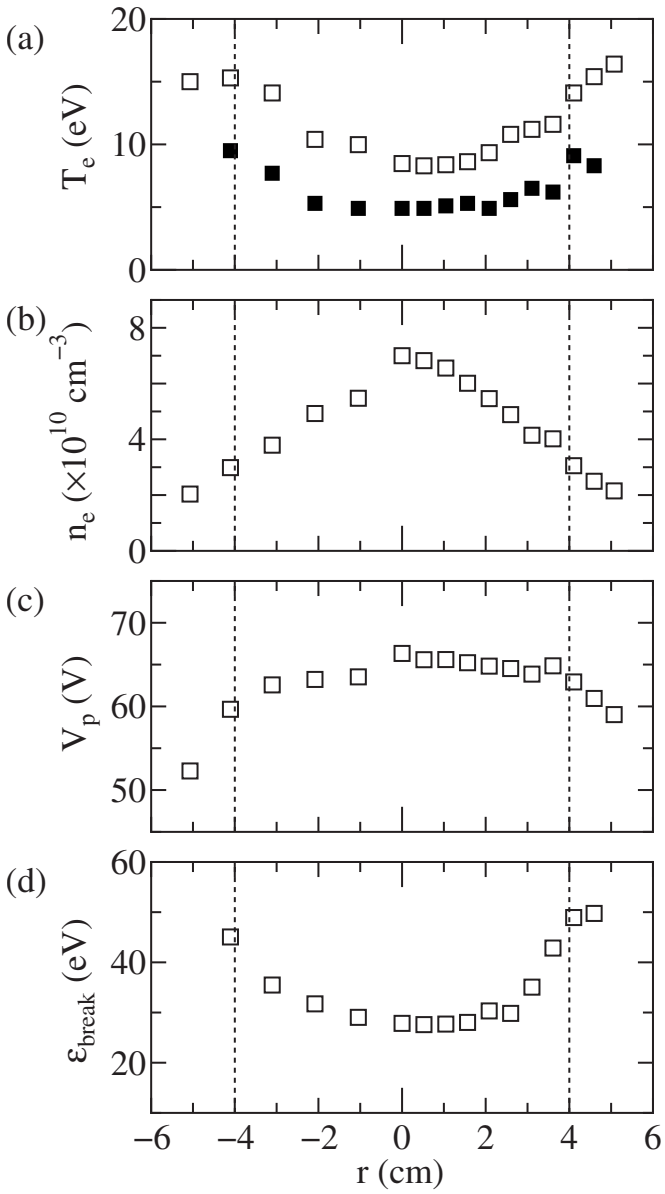

FIG. 3. (a) Electron temperature $T_{e\ \mathrm{bulk}}$ (open square) and $T_{e\ \mathrm{tail}}$ (black square), (b) electron density n_e, (c) plasma potential V_p, and (d) the break energy $\varepsilon_{\mathrm{break}}$ measured across the source diameter using the rf compensated Langmuir probe placed at $z=17$ cm; operating conditions are 250 W rf power and 0.3 mTorr gas pressure.

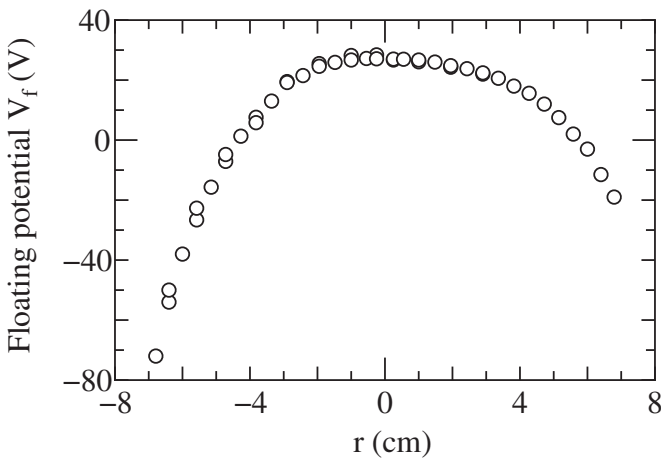

FIG. 4. Floating potential measured across the source diameter using a noncompensated Langmuir probe placed at $z=17$ cm.

trapped and escaping), density n_e, plasma potential V_p, and break point energy $\varepsilon_{\mathrm{break}}$ as a function of the helicon source radius are shown in Figs. 3(a)–3(d), respectively. The inner region ($r<2$) shows a quasiconstant V_p, $\varepsilon_{\mathrm{break}}$, $T_{e\ \mathrm{bulk}}$, and $T_{e\ \mathrm{tail}}$, whereas for radii beyond about 4 cm, which is close to the magnetic field line that passes through the greatest estimated radial extent of the DL at $z=25$ cm, increased values of $\varepsilon_{\mathrm{break}}$, $T_{e\ \mathrm{bulk}}$, and $T_{e\ \mathrm{tail}}$ can be seen along with a decrease of the plasma potential near the wall. In between these two regions the parameters change rather smoothly. It is tempting to suggest that the difference between these two regions is a result of electrons in the outer regions being heated along field lines that terminate on the insulating walls of the source and those in the inner regions that have axial boundary conditions determined by the double layer and the diffusion chamber. The plasma density shows a triangular radial variation which we would consider representative of a primary ionization mechanism in the center (probably due to the helicon wave) coupled with good radial confinement of the electrons, which is not surprising considering the mean free path for electron neutral collisions is about 100 cm. The ratio of $T_{e\ \mathrm{bulk}}$ to $T_{e\ \mathrm{tail}}$ appears constant and equal to about 1.5 across both the inner and outer regions; the reason for this is not yet clear. In previous publications on both experiment[11] and simulation[10] we have hypothesized that the high $T_{e\ \mathrm{bulk}}$ relative to the $T_{e\ \mathrm{tail}}$ is due to the trapped electrons experiencing the heating fields of the rf antenna more often than the free electrons. The electron heating mechanism is rather complicated as the rf inductive fields will be higher nearer the antenna resulting in a more rapid transfer of energy in that region from the rf fields to the electrons. In the simplest possible model, the field from the antenna drops away with an e-folding length of $\delta=c/\omega_{pe}$, where c is the velocity of light and ω_{pe} is the electron plasma frequency; as an example, $\delta\sim 5.3$ cm for a plasma density of 10^{10} cm^{-3}. The plasma density for the present experiments has a maximum value on axis at $z=17$ cm of 7×10^{10} cm^{-3},[6] and decreases to about 2×10^{10} cm^{-3} near the wall. Hence we would expect a δ ranging from 3.8 cm near the wall to 2 cm in the center.

In a previous publication[23] we have shown that large negative potentials have been detected using a floating probe in the plasma close to one of the straps of the helicon antenna. It was hypothesized that this is due to the glass insulating wall charging up negatively as initially demonstrated by Butler and Kino.[24] This phenomenon is very similar to the charging up of the series (tune) capacitor in a matching network resulting in a negative bias on an immersed electrode in a capacitively coupled rf plasma system. This effect has also been integrated in a power deposition model of a small diameter nonmagnetized helicon source and successfully compared to experimental results.[25]

The radial variation of the floating potential V_f obtained using a 1 mm in diameter non-rf compensated planar Langmuir probe also placed at $z=17$ cm is shown in Fig. 4 and is interesting for two very obvious phenomena. The first is that

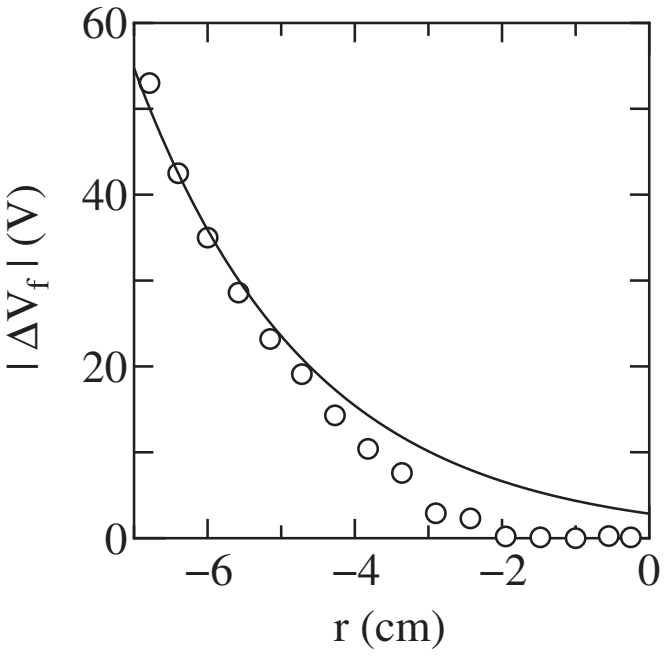

FIG. 5. Open circles are the difference $|\Delta V_f|$ between the left and right measured V_f of Fig. 4, and the solid line is an exponential fit having an e-folding of 2.4 cm.

V_f is highly negative at the plasma source walls. The second is the clear asymmetry with the negative radial values seeming to have an extra imposed radially dependent negative potential. Surrounding the source is a rf double saddle field helicon antenna[25] and the dog-leg probe used for the V_f measurements comes to within about 2 cm of the antenna on the left-hand side of Fig. 4 and within 4 cm on the right-hand side of Fig. 4. Hence we would expect that there would be greater influence on the floating potential on the left-hand side than on the right-hand side. In order to get an idea of this influence, the values of the V_f on the right-hand side are subtracted from the corresponding values on the left-hand side; the result $|\Delta V_f|$ is shown in Fig. 5. The fit is fairly good and represents the skin depth for a simple plasma having a density of 5×10^{10} cm^{-3} equal to the geometrical mean of the measured plasma density. The above discussion is obviously very approximate but it shows that the majority of the measurements are internally coherent and it is possible to assign a reasonable degree of confidence to the EEPF measurements (which are very difficult to verify using other techniques).

The experiments show a clear difference between the plasma that is connected to the DL and the downstream plasma by the magnetic field and the plasma that is permeated by magnetic field lines that terminate in the source region. These two regions are separated by a radial extent of a couple of centimeters which shows some characteristics of both regions. In the former case, the EEPFs show a fairly constant $T_{e\ \mathrm{bulk}}$ and $T_{e\ \mathrm{tail}}$ as a function of radius and the break energy between the two distributions corresponds well with the potential drop of the DL. Additionally, the value of the potential drop of the DL corresponds well with $5\times T_{e\ \mathrm{tail}}$ suggesting that the DL is effectively a terminating wall for the source plasma where the flux of ions and electrons escaping through the DL is equal. In the latter, the electrons near the wall on magnetic field lines that intersect the wall have a much higher $T_{e\ \mathrm{bulk}}$ and $T_{e\ \mathrm{tail}}$, although the ratio between $T_{e\ \mathrm{bulk}}$ and $T_{e\ \mathrm{tail}}$ for both situations remains at about 1.5. Radial measurements of the floating potential suggest that the field of the rf antenna penetrates radially into the source with a skin depth approximately given by the simple formula for unmagnetized plasmas. These high fields near the wall would be the reason for the higher electron temperatures. Once again, the break energy appears to correspond to the sheath potential at the wall, as a result of the requirement for equal fluxes of positive and negative species.

[1] S. A. Cohen, N. S. Siefert, S. Stange, R. F. Boivin, E. E. Scime, and F. M. Levinton, Phys. Plasmas **10**, 2593 (2003).
[2] C. Charles and R. W. Boswell, Appl. Phys. Lett. **82**, 1356 (2003).
[3] X. Sun, A. M. Keesee, C. Biloiu, E. E. Scime, A. Meige, C. Charles, and R. W. Boswell, Phys. Rev. Lett. **95**, 025004 (2005).
[4] C. Biloiu, X. Sun, E. Choueiri, F. Doss, E. Scime, J. Heard, R. Spektor, and D. Ventura, Plasma Sources Sci. Technol. **14**, 766 (2005).
[5] N. Plihon, P. Chabert, and C. S. Corr, Phys. Plasmas **14**, 013506 (2007).
[6] C. Charles and R. W. Boswell, Appl. Phys. Lett. **91**, 201505 (2007).
[7] R. E. Ergun, Y.-J. Su, L. Andersson, C. W. Carlson, J. P. McFadden, F. S. Mozer, D. L. Newman, M. V. Goldman, and R. J. Strangeway, Phys. Rev. Lett. **87**, 045003 (2001).
[8] R. W. Boswell, E. Marsch, and C. Charles, Astrophys. J. Lett. **640**, L199 (2006).
[9] C. Charles, R. W. Boswell, and M. A. Lieberman, Appl. Phys. Lett. **89**, 261503 (2006).
[10] A. Meige and R. W. Boswell, Phys. Plasmas **13**, 092104 (2006).
[11] K. Takahashi, C. Charles, R. W. Boswell, T. Kaneko, and R. Hatakeyama, Phys. Plasmas **14**, 114503 (2007).
[12] V. A. Godyak, R. B. Piejak, and B. M. Alexandrovich, Plasma Sources Sci. Technol. **11**, 525 (2002).
[13] M. A. Lieberman and C. Charles, Phys. Rev. Lett. **97**, 045003 (2006).
[14] M. A. Lieberman, C. Charles, and R. W. Boswell, J. Phys. D **39**, 3294 (2006).
[15] A. Aanesland, C. Charles, M. A. Lieberman, and R. W. Boswell, Phys. Rev. Lett. **97**, 075003 (2006).
[16] C. Charles, Appl. Phys. Lett. **84**, 332 (2004).
[17] A. Fruchtman, Phys. Rev. Lett. **96**, 065002 (2006).
[18] F. F. Chen, Phys. Plasmas **13**, 034502 (2006).
[19] I. A. Biloiu, E. E. Scime, and C. Biloiu, Appl. Phys. Lett. **92**, 191502 (2008).
[20] C. Charles and R. W. Boswell, Phys. Plasmas **11**, 1706 (2004).
[21] C. Charles, Plasma Sources Sci. Technol. **16**, R1 (2007).
[22] M. A. Lieberman and A. J. Lichtenberg, *Principle of Plasma Discharges and Materials Processing*, 2nd ed. (Wiley-Interscience, Hoboken, 2005), p. 172.
[23] A. Aanesland, C. Charles, R. W. Boswell, and A. Fredriksen, Plasma Sources Sci. Technol. **12**, 85 (2003).
[24] H. S. Butler and G. S. Kino, Phys. Fluids **6**, 1346 (1963).
[25] C. Charles, R. W. Boswell, and M. A. Lieberman, Phys. Plasmas **10**, 891 (2003).